ARTICLES

Electronic and magnetic properties of layered colossal magnetoresistive oxides: $La_{1+2x}Sr_{2-2x}Mn_2O_7$

X. Y. Huang, O. N. Mryasov, D. L. Novikov, and A. J. Freeman
Department of Physics and Astronomy, Northwestern University, Evanston, Illinois 60208
(Received 13 April 2000)

The electronic and magnetic properties of double-layered Roddlesdon-Popper compounds, $La_{1+2x}Sr_{2-2x}Mn_2O_7$ with different doping x from 0.0 to 0.2 have been calculated using the full-potential linear muffin-tin orbital method. The total energies, band structures, densities of states, and Fermi surfaces were investigated by means of the virtual crystal approximation. The band structure of $La_{1+2x}Sr_{2-2x}Mn_2O_7$ is found to be that of a half-metallic ferromagnet, in agreement with experiment. The density of states shows that La and Sr act solely as electron donors and have almost no states at or below the Fermi level, and therefore a rigid band approximation can be considered as a good approximation to describe the effects of doping. The calculated Mn magnetic moments increase from $3.09\mu_B$ to $3.24\mu_B$ when the doping increases from 0.0 to 0.2, which is in qualitative agreement with experiment. The calculated Fermi surface shows pronounced nesting features along the Γ-X directions in the undoped case, which implies a possible charge- or spin-density wave instability in this material.

There is considerable research interest in the double-layered Roddlesdon-Popper compounds $La_{1+2x}Sr_{2-2x}Mn_2O_7$, where x is the electron doping in the Mn-O planes.[1,2] This material is comprised of perovskite double layers of corner-linked MnO_6 octahedra forming infinite sheets, and double layers of $(La,Sr)MnO_3$ that are separated along the c axis by insulating (La,Sr)O layers. With proper doping, this kind of manganite exhibits intrinsic colossal magnetoresistance (CMR) associated with a phase transition from a high-temperature paramagnetic and insulating phase to a low-temperature ferromagnetic and metallic phase. Such anomalous magnetotransport behavior in perovskite materials is usually explained on the basis of Zener's double-exchange concept,[3–5] which has been recently modified to take into account lattice Jahn-Teller distortions[6] characterstic for these materials.[7–9] In contrast, the double-layered manganites show very small lattice distortions.[10,11] The existence of insulating (La,Sr)O layers in this layered system makes its physical properties strongly anisotropic. This material is also important and interesting due to its pronounced CMR in low field.[2]

The investigation of electronic structure is important in providing a better understanding of the physics of this kind of quasi-two-dimensional (quasi-2D) manganite. Unlike perovskite manganites, this kind of material provides a rich opportunity to explore structure-property relationships on varying length and time scales in reduced dimensions. Clearly, understanding both is an essential ingredient in developing an overall picture of the physics of this class of transition metal oxides. Very recently, neutron-powder diffraction and Rietveld analyses carried out by Kubota *et al.*[12] provided the structural parameters of $La_{1.2}Sr_{1.8}Mn_2O_7$ at low temperature, which make it possible for us to investigate these manganites in detail.

Papers on the electronic structure of these double-layered manganites are few and have only recently appeared. In 1998, a study based on the local spin density approximation with a Coulomb correction (LSDA + U) was reported for the electronic structure of $La_{1.2}Sr_{1.8}Mn_2O_7$ with a doping of 0.1

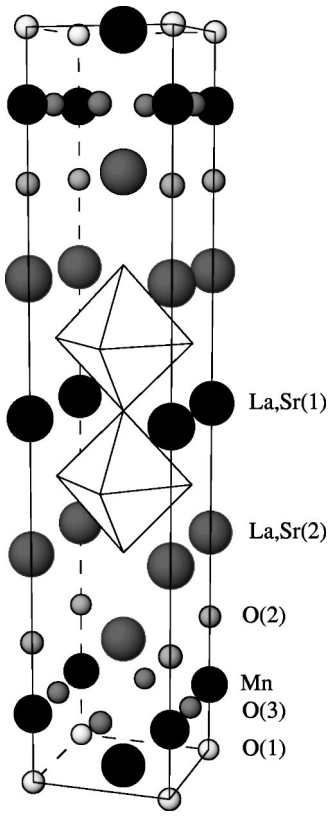

FIG. 1. Crystal structure of $La_{1+2x}Sr_{2-2x}Mn_2O_7$.

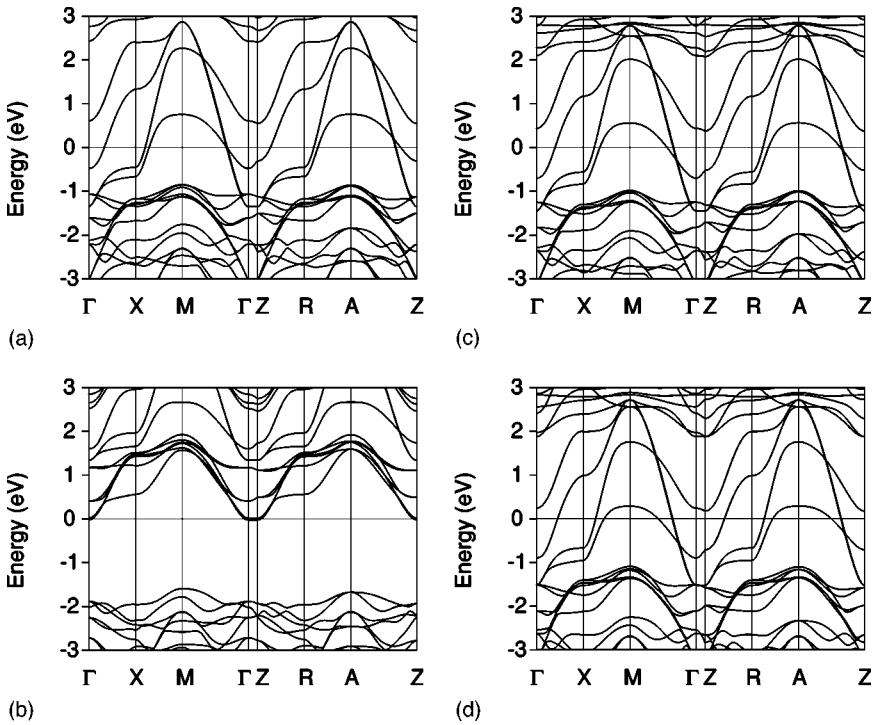

FIG. 2. Band structure results for $La_{1+2x}Sr_{2-2x}Mn_2O_7$ along symmetry lines in the simple tetragonal BZ: (a) majority and (b) minority spins for $x=0.0$, (c) majority spin for $x=0.1$, and (d) majority spin for $x=0.2$.

by Dessau *et al.*[13] They showed a relatively good agreement between theory and their experiment. In 1999, a first-principles calculation based on density-functional theory within the generalized gradient approximation was reported on $LaSr_2Mn_2O_7$ by de Boer and de Groot.[14] However, their work was focused on only the undoped case and no Fermi surface is presented. Thus further investigations are needed to understand more about the effects of the doping and the anisotropic character of the transport properties and 2D-like nature of the magnetism.

In this paper, we give a detailed description of the electronic structure of double-layered manganites $La_{1+2x}Sr_{2-2x}Mn_2O_7$ for La doping in the range of $0.0 \leqslant x \leqslant 0.2$ using the first-principles local density full-potential linear muffin-tin orbital (FLMTO) method.[16–19] We focus on (i) the determination of the dependence of the band structures and Fermi surfaces on La doping, and (ii) the intrinsic reason for existence of charge ordering in the undoped manganite.

The calculations were carried out in the spin-polarized scalar-relativistic mode within the Ceperly-Alder form of exchange-correlation potential. In our calculations for $La_{1+2x}Sr_{2-2x}Mn_2O_7$, no shape approximations are made to either the density or potential. We used a triple-κ basis set for each type of atom and each angular momentum l-channel with kinetic energies of -0.01, -1.0, and -2.3 Ry. Nonoverlapping muffin-tin spheres were chosen in our calculations. No empty spheres were introduced since the space filling is over 50%. The Brillouin zone integrations were carried out by the tetrahedron method using a 75 k-point

TABLE I. Results of equilibrium volumes calculated for different doping levels.

Doping level x	0.00	0.02	0.05	0.10	0.15	0.20
$V(x)/V_0(x)$	0.971	0.973	0.975	0.974	0.975	0.963

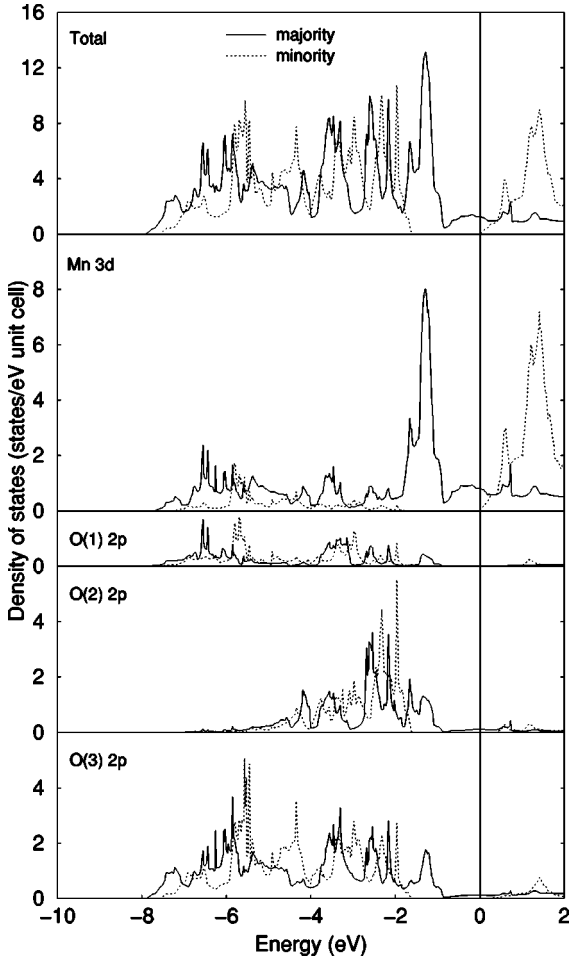

FIG. 3. Total and projected densities of states of Mn and O for $LaSr_2Mn_2O_7$, where the vertical solid line denotes E_F.

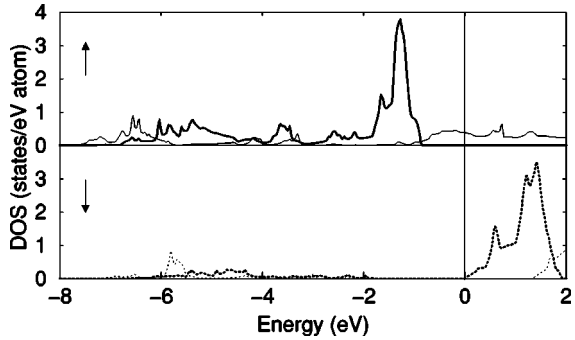

FIG. 4. Projected Mn $3d$ densities of states for $LaSr_2Mn_2O_7$. Thick and thin lines represent the t_{2g} and e_g states, respectively. The vertical solid line denotes E_F.

mesh (corresponding to $8\times8\times8$ regular divisions along the k_x, k_y, and k_z axes) in the $\frac{1}{16}$ irreducible wedge. The local orbital[20] method was used to treat the semicore states of La $5s$, $5p$, Sr $4s$, $4p$, and Mn $3p$. Finally, the virtual crystal approximation (VCA) was used to investigate the role of

TABLE II. Partial O $2p$ DOS (states/eV atom) for $LaSr_2Mn_2O_7$ at E_F.

Atom	p	p_x	p_y	p_z
O(1)	0.020	0.003	0.003	0.014
O(2)	0.092	0.001	0.001	0.090
O(3)	0.047	0.022	0.022	0.003

doping level x from 0.0 to 0.2 in the Sr sublattice, which is modeled by placing a nuclear charge of $Z_{VC}=38+x$ at each Sr site. This VCA approach allows a self-consistent treatment of the change in charge densities and carrier densities.

$La_{1+2x}Sr_{2-2x}Mn_2O_7$ occurs in the body-centered tetragonal structure which has $I4/mmm$ space group symmetry. As shown in Fig. 1, the Mn atoms are coordinated above and below by the apical O(1) atoms in the double (La,Sr)-O layers. Assuming completely ionic character, Mn atoms would be in d^4 and d^3 configurations. Unlike the 3D perovskite systems, where the Jahn-Teller distortion is very common below the insulator-metal transition, this layered manganite

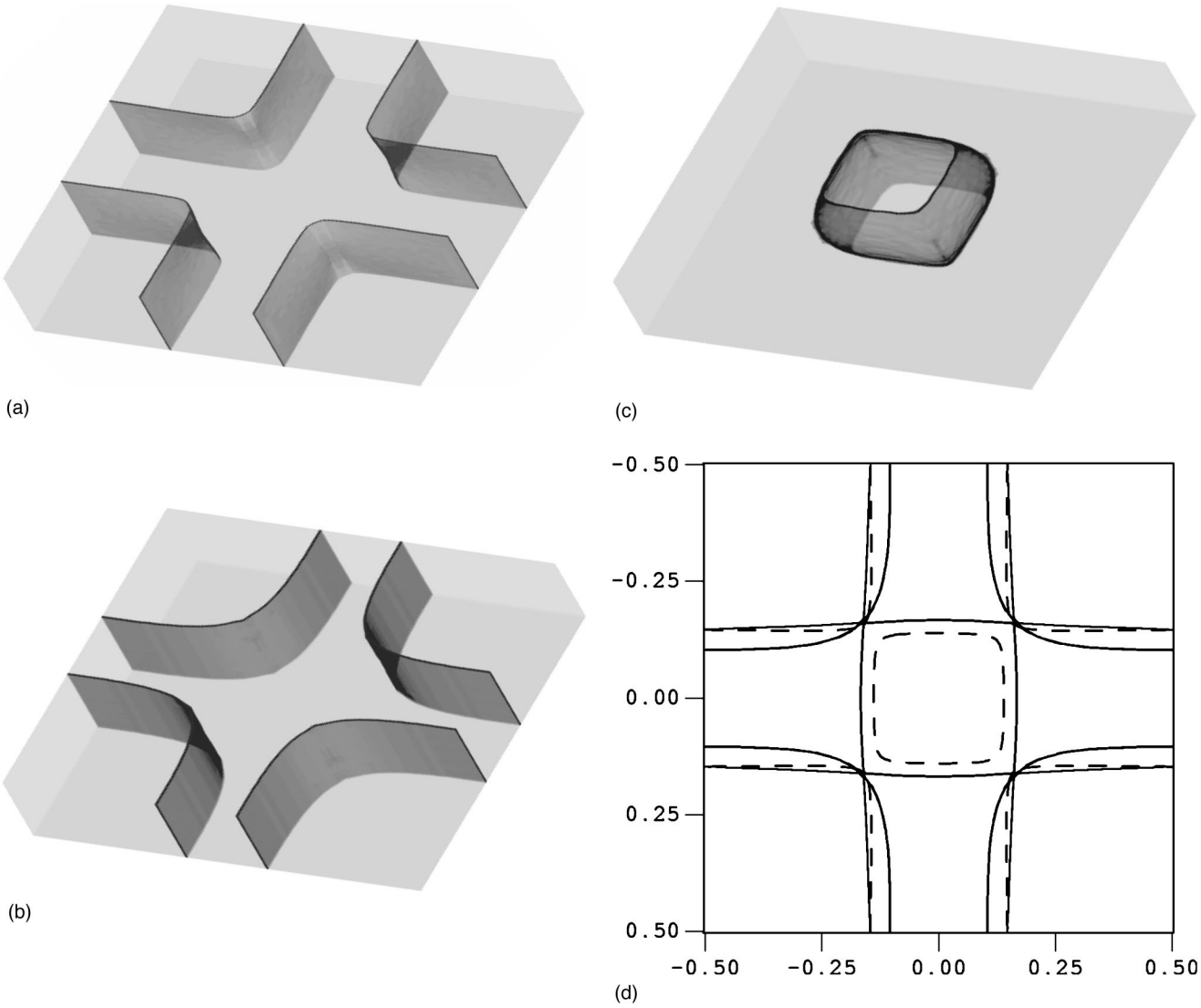

FIG. 5. Fermi surfaces of majority spin for $LaSr_2Mn_2O_7$: (a), (b), (c) in the 3D BZ and (d) in the Γ-X-M plane (solid line) and Z-R-A plane (dashed line).

TABLE III. The total magnetic moment (M_{tot}) and magnetic moment per Mn site (M_{Mn}) in μ_B for ferromagnetic $LaSr_2Mn_2O_7$ with different La doping levels.

	Doping level					
	0.00	0.02	0.05	0.10	0.15	0.20
M_{tot}	7.00	7.04	7.10	7.19	7.27	7.35
M_{Mn}	3.090	3.096	3.122	3.164	3.195	3.238
M_{Mn}^{expt}			3.1[a]	3.2[a]		

[a]Data from Ref. 12.

exhibits very small lattice distortions—which may give rise to a different electronic structure. The lattice parameters used in our calculations are taken from the neutron studies by Kubota *et al.*;[12] these are different from those used in de Boer and de Groot's calculations.[14]

Total energy calculations were performed for a set of different unit cell volumes ($V/V_0=1.0,0.98,0.96,0.94,0.92$), where V_0 is the experimental volume. The optimization is obtained by finding the minimum energy for each doping. The resulting equilibrium volumes are listed in Table I. As seen, our theoretical values differ from experiment[12] in the range between -2.5% and -3.7%. The largest discrepancy of -3.7% comes from a doping of 0.2. This is reasonable because we have not considered the atomic size of La in the doping cases.

The electronic band structure of the manganites with a La doping of 0.0, 0.1, and 0.2 is shown in Fig. 2 along some high symmetry lines in the simple tetragonal Brillouin zone (BZ), where $X=(\pi/a,0,0)$, $M=(\pi/a,\pi/a,0)$, $Z=(0,0,\pi/c)$, $R=(\pi/a,0,\pi/c)$ and $A=(\pi/a,\pi/a,\pi/c)$. The total and projected densities of states (DOS's) for the different atoms inside their muffin-tin spheres are displayed in Fig. 3 for the undoped $LaSr_2Mn_2O_7$ case.

As seen, the band structure with different doping is a half-metallic ferromagnet due to a band gap within the Mn minority spin *d* bands of about 1.7–1.9 eV. The Mn *d* bands are strongly dispersive, and not flat and narrow as are those in an ionic insulator. Doping La into $LaSr_2Mn_2O_7$ can cause an upward shift of E_F since La acts as an electron donor in these manganites. The band structure near E_F is strongly anisotropic, with little *c*-axis dispersion, which can be seen clearly from the small dispersions along the short Γ-Z direction. From an ionic analysis the bands below E_F are expected to contain 42 O $2p$ electrons and 7 Mn $3d$ electrons for a total of 24 bands. This picture is only approximately correct since the O(2) and O(3) atoms have open shell character. The band crossing E_F along the Γ-X direction is identified to have primarily $d_{x^2-y^2}$ in-plane character, while the other two bands crossing E_F along the X-M direction have $d_{3z^2-r^2}$ character.

Strong hybridization between Mn and O is also seen clearly through both the similar shapes of the Mn and O projections of the DOS below E_F and the in-plane dispersions of the energy bands. E_F is located in the Mn e_g manifold (see Fig. 4), which indicates that Mn^{3+} and Mn^{4+} have high-spin states in this compound. Unlike for $LaMnO_3$,[21] there is no gap between the hybridized t_{2g} and e_g manifolds in either the majority on minority channel. It is worth noting that the DOS for $LaSr_2Mn_2O_7$ is very similar to that for

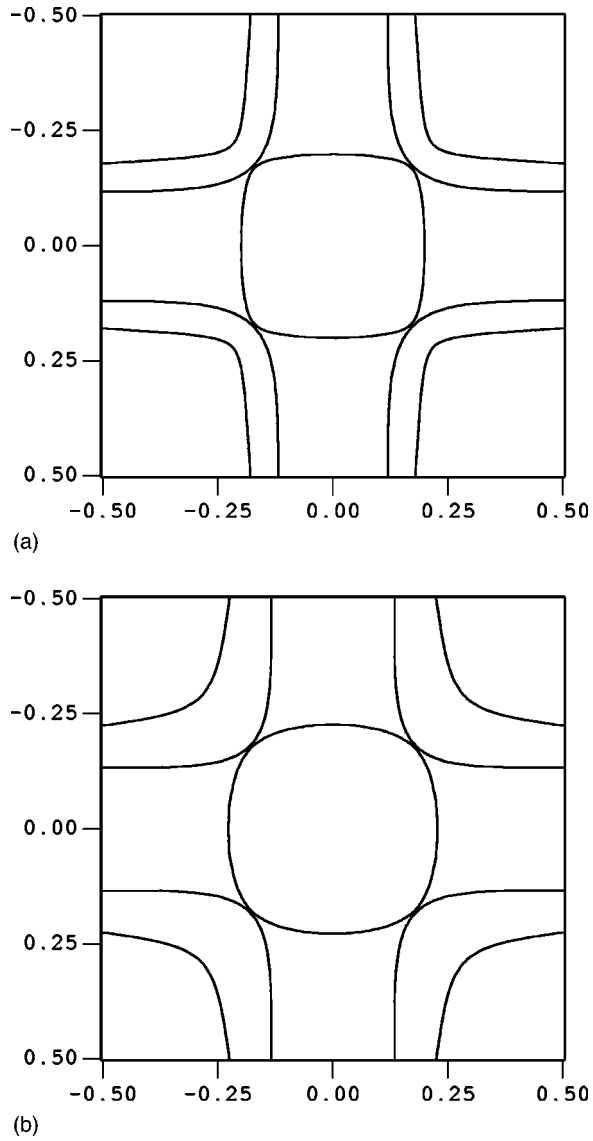

FIG. 6. Fermi surfaces of majority spin for $La_{1+2x}Sr_{2-2x}Mn_2O_7$ in the Γ-X-M plane with doping levels of (a) 0.1 and (b) 0.2.

cubic ferromagnetic $LaMnO_3$.[21] In $LaMnO_3$, due to a strong Jahn-Teller distortion and a rotation, the Mn-O-Mn bond angles are changed from 180° to ~160°, which results in less favorable hopping between the t_{2g} and e_g manifolds. However, the 180° bond angles in $LaSr_2Mn_2O_7$ are not changed by distortion; therefore, hopping between the t_{2g} and e_g states in this manganite is more favorable than that in $LaMnO_3$ and no new gaps are opened. The Mn t_{2g} state is quite localized and forms a magnetic moment of $2.5\mu_B$, while the Mn e_g state crosses E_F and forms the conduction bands with a Mn magnetic moment of about $0.6\mu_B$. We decomposed the O p DOS at E_F into the p_x, p_y, and p_z components listed in Table II. Note that the conduction band contribution at E_F is mainly from O(1) and O(2) p_z and from O(3) p_x and p_y, which clearly shows the anisotropic nature of the conduction electrons.

It is interesting to note that the total DOS near E_F comes mainly from Mn and O; there are almost no contributions from La and Sr. That is to say, in these compounds La and Sr atoms act solely as electron donors and small changes of La

or Sr concentrations would not change any major features of the band structure. Therefore, a rigid band approximation can be considered as a good approximation to describe the effects of doping. The (La,Sr)O layers almost have an insulating behavior in this material.

Now, we turn to check the magnetic properties vs doping. The total magnetization and magnetization per Mn site with different doping levels from 0.0 to 0.2 are listed in Table III. With increasing doping, the Mn magnetic moment increases from $3.09\mu_B$ to $3.24\mu_B$, which is in qualitative agreement with experiment. In the calculation of de Boer and de Groot,[14] the magnetic moment per unit cell for the undoped case is $6.995\mu_B$ which is identical to our LSDA results. However, the magnetic moment per Mn site is slightly smaller than ours. This is because the Mn muffin-tin radii adoped in their calculations were smaller than ours.

The Fermi surfaces for the undoped case are shown in Fig. 5. It can be seen that the free-electron-like bands crossing E_F give rise to quite simple Fermi surfaces, which consist of three cylindrical sheets, one of which is an electronlike square cylinder centered at Γ and characterized primarily by $d_{3z^2-r^2}$ symmetry, and the other two holelike cylinders centered at M, characterized by $d_{x^2-y^2}$ symmetry. These three bands are degenerate at $(\pi/3a,\pi/3a)$ in the Γ-X-M plane. The three Fermi surfaces are open in the Γ-Z direction, reflecting the layered crystal structure and a nearly 2D property.

The Fermi surfaces show pronounced nesting features along the Γ-X directions with nesting vectors in the range between $(0.20\pi/a,0,0)$ and $(0.33\pi/a,0,0)$. This pronounced nesting suggests a possible charge- or spin-density wave instability (CDW/SDW) with nearly commensurate periodicity $\pm(3a,0)$, $\pm(4a,0)$ or $\pm(5a,0)$ in planes perpendicular to Γ-Z. Our result suggests that such an instability would account for the $d_{3x^2-r^2}/d_{3y^2-r^2}$ orbital ordering of Mn^{3+} and Mn^{4+} in this manganite.[15]

This situation will change when doping is introduced. The Fermi surfaces for the doped cases of 0.1 and 0.2 are shown in Figs. 6(a) and (b), respectively. Two major changes can be seen clearly by comparing Fig. 5 and Fig. 6: first, the sheet of the central square expands outward and becomes round; second, two $d_{x^2-y^2}$ bands shift outward from Γ and their degeneracy is eliminated. The Fermi surfaces for the doped case are therefore similar to those determined by Dessau *et al.*,[13] but there is degeneracy along Γ-X between the $d_{3z^2-r^2}$ band and one of the $d_{x^2-y^2}$ bands. Consequently, the nesting features are no longer as strong as in the undoped case. In fact, no charge ordering phenomena have been observed in the doped cases.

In conclusion, we performed total energy full-potential LMTO calculations to determine the electronic structure and Fermi surfaces of the double-layered manganite, $La_{1+2x}Sr_{2-2x}Mn_2O_7$. The electronic structure results show that this manganite is a half-metallic ferromagnet. The DOS near E_F is composed mainly of Mn states. The La and Sr atoms act simply as electron donors and so a rigid band approximation can work well for describing the effects of doping. Pronounced Fermi surface nesting features were found in the undoped case with little dispersion in the Γ-Z direction, which may give rise to a CDW or SDW instability. Since the Fermi surfaces are of very strong Mn $3d$ character, the resulting CDW or SDW will involve the Mn atoms. We believe that the Fermi surface nesting accounts for the charge ordering observed in this manganite.

This work was supported by the Department of Energy (Grant No. DE-F602-88ER45372) and by a grant of computer time at NERSC.

[1] Y. Moritomo, A. Asamitsu, H. Kuwahara, and Y. Tokura, Nature (London) **380**, 141 (1996).
[2] J. F. Mitchell, D. N. Argyriou, J. D. Jorgensen, D. G. Hinks, C. D. Potter, and S. D. Bader, Phys. Rev. B **55**, 63 (1997).
[3] C. Zener, Phys. Rev. **82**, 403 (1951).
[4] P. W. Anderson and H. Hasegawa, Phys. Rev. **100**, 675 (1955).
[5] P. G. de Gennes, Phys. Rev. **118**, 141 (1960).
[6] A. J. Millis, P. B. Littlewood, and B. I. Shraiman, Phys. Rev. Lett. **74**, 5144 (1995).
[7] J. H. Vleck, J. Chem. Phys. **7**, 72 (1939).
[8] J. Kanamori, Jpn. J. Appl. Phys., Suppl. **31**, 14s (1960).
[9] K. I. Kugel and D. I. Khomskii, Usp. Fiz. Nauk **25**, 231 (1982) [Sov. Phys. Usp. **25**, 231 (1982)].
[10] T. G. Perring, G. Aeppli, Y. Moritomo, and Y. Tokura, Phys. Rev. Lett. **78**, 3197 (1997).
[11] D. N. Argyriou, J. F. Mitchell, J. B. Goodenough, O. Chmaissem, S. Short, and J. D. Jorgensen, Phys. Rev. Lett. **78**, 1568 (1997).
[12] M. Kubota, H. Fujioka, K. Hirota, K. Ohoyama, Y. Moritomo, H. Yoshizawa, and Y. Endoh, ISSP Technical Report, Ser. A, No. 3459, 1999 (unpublished).
[13] D. S. Dessau, T. Saitoh, C.-H. Park, Z.-X. Shen, P. Villella, N. Hamada, Y. Moritomo, and Y. Tokura, Phys. Rev. Lett. **81**, 192 (1998).
[14] P. K. de Boer and R. A. de Groot, Phys. Rev. B **60**, 10 758 (1999).
[15] J. Q. Li, Y. Matsui, T. Kimura, and Y. Tokura, Phys. Rev. B **57**, R3205 (1998).
[16] M. Methfessel, Phys. Rev. B **38**, 1537 (1988).
[17] M. Methfessel, C. O. Rodriguez, and O. K. Andersen, Phys. Rev. B **40**, 2009 (1989).
[18] A. T. Paxton, M. Methfessel, and H. Polatoglu, Phys. Rev. B **42**, 8127 (1990).
[19] M. Methfessel and M. Scheffler, Phys. Rev. B **43**, 175 (1991).
[20] D. J. Singh, *Planewaves, Pseudopotentials, and the LAPW Method* (Kluwer Academic, Boston, 1994).
[21] D. J. Singh and W. E. Pickett, Phys. Rev. B **57**, 88 (1998).